Applicability of the Ohmic Model for voltammetric growth of ZnO on galvanized steel sheets containing Sb or Pb

Aplicabilidade do Modelo Ôhmico para o crescimento voltamétrico de ZnO sobre folhas de aço galvanizado contendo Sb ou Pb

Aplicabilidad del Modelo Óhmico el crecimiento voltamétrico de ZnO sobre hojas de acero galvanizado que contiene Sb o Pb

Tiago Brandão Costa
ORCID: https://orcid.org/0000-0003-3028-7965
Universidade Federal Fluminense, Brazil
E-mail: tiagobrandao@id.uff.br
Tania Maria Cavalcanti Nogueira
ORCID: https://orcid.org/0000-0001-7583-6820
Universidade Federal Fluminense, Brazil
E-mail: tania@veleiro.net

Abstract
The aim of this study was to verify the applicability of the Ohmic Model with variable ionic resistivity to the voltammetric zinc oxide growth on galvanized steel sheets, without chromate passivating film. Two kind of galvanized steel sheets were studied: one produced from a bath of molten zinc containing antimony and the other containing lead. The galvanized steel sheets produced from a bath containing Sb presented better performance against corrosion in comparison on with those produced from a bath containing Pb. The electrochemical experiments were performed in a buffer solution of pH 8.7 with of 0.3 mol L^{-1} H$_3$BO$_3$ plus 0.15 mol L^{-1} Na$_2$B$_4$O$_7$. It was found that the passivating zinc oxide grown on the galvanized steel sheet containing Sb showed higher ionic resistivity than that of the galvanized sheet containing Pb. This can explain the corrosion results.
Keywords: Zinc oxide; Galvanized steel sheet; Ohmic model.

Resumo
O objetivo desse estudo foi verificar a aplicabilidade do Modelo Ohmico com Resitividade iônica variável para o crescimento de óxidos de zinco sobre folhas de aços galvanizadas, sem filme de passivação de cromato. Dois tipos de folhas de aço galvanizadas foram estudadas: uma produzida com banho de zinco contend antimônio e a outra contendo chumbo. Esses dois tipos de folhas tem distintos comportamentos frente à corrosão, as com antimônio apresentam melhor performance. Os experimentos foram realizados em solução tampão borato pH 8,7 com 0,3 mol L^{-1} H$_3$BO$_3$ adicionado 0,15 mol L^{-1} Na$_2$B$_4$O$_7$. Observou-se que os óxidos de zinco passsivados sobre a folha de aço galvanizada contendo Sb mostraram maior resistência ionic do que as folhas galvanizadas contendo Pb.
Palavras-chave: Óxido de zinco; Folhas de aço galvanizadas; Modelo ôhmico.

Resumen
El objetivo de este estudio fue verificar la aplicabilidad del Modelo Óhmico con resistividad iónica variable para el crecimiento de óxidos de zinc sobre hojas de acero galvanizado, sin película de pasivación de cromato. Dos tipos de hojas de acero galvanizado fueron estudiadas: una producida con baño de zinc que contiene antimonio y la otra que contiene plomo. Estos dos tipos de hojas tienen diferentes comportamientos frente a la corrosión, las hojas con antimonio presentaron un major rendimiento. Los experimentos se realizaron en solución tampón borato pH 8,7 con 0,3 mol L^{-1} H$_3$BO adicionado 0.15 mol L^{-1} Na$_2$B$_4$O$_7$. Se observó que los óxidos de zinc pasivados en la hoja de acero galvanizado que contiene Sb tuvieron una resistencia iónica más grande que las hojas galvanizadas que contienen Pb.
Palabras clave: Óxido de zinc; Hojas de acero galvanizado; Modelo óhmico.

1. Introduction

Steel can provide adequate mechanical properties in many applications, although when in contact with humid air at high temperatures it corrodes. For this reason, very often, steel surface is coated with different metals more resistant to

corrosion. Zinc is one of the most used metals used as coating to steel surfaces. It acts as a barrier against corrosive media, providing galvanic protection (Marder, 2000).

The hot-dip galvanizing process is one of the most used to coat steel sheets with zinc. In this case steel is dipped in a bath of molten zinc containing some binders as aluminum, antimony or lead. Aluminum is added to the bath in order to inhibit the reaction between iron and zinc. Lead or antimony are usually incorporated into the zinc bath to induce an increase in the bath fluidity and a decrease in its surface tension. In small concentrations (0.04 – 0.2% in weight) these elements improve the zinc coating uniformity and its adhesion to the steel substrate. Furthermore, they also contribute to the zinc crystals nucleation. Some studies show that Sb and Pb modify the coating texture and the composition of the surfaces (Cameron, Ormay, 1965) (Seré, et al., 1999) (Asgari, et al., 2007) (Asgari, et al., 2009. These phenomena affect not only the zinc coating texture but also its surface appearance and corrosion resistance. Frequently, antimony is present within the coating while lead can be found fundamentally at the zinc surface (Seré, et al., 1999; Chang & Shin, 1994; Brogueira, 2008).

Besides all this, the influence of these elements in the zinc oxide growth is still not well elucidated. In fact, studies which evaluate the corrosion resistance of hot-dip galvanized steel sheets in aqueous solutions are carried out by electrochemical techniques which analyze the metal/film/solution interface as a whole. Many authors use potentiostatic polarization technique to obtain the corrosion current density (i_{corr}) by the extrapolation of the Tafel plots (Tomachuk, Melo, & Bellucci, 2006; Kobayashi & Fujiwara, 2006. Hosseini, et al., 2007; Lin, et al., 2007; Fedel, et al., 2009; Meng, et al., 2009; Hamlaoui, et al., 2009; Ramezanzadeh, et al., 2010; Taouil, et al., 2012). In this case, the i_{corr} values are a result of the passivating current densities through the metal/film/solution interface, without the separation of the properties between the metal/film interface and the film itself. On the other hand, electrochemical impedance techniques analyze the system in terms of equivalent electrical circuits, which can be the object of different criticisms.

The aim of the present work was to study the voltammetric growth of zinc oxide on hot-dip galvanized steel sheets containing Sb or Pb in the coating in a way to separate the contributions of the metal/film interface from that of the film. In this work, the quantitative scientific research method was used (Pereira, et al., 2018). This method generates data that can be analyzed by generation equation and/or mathematical formulas applicable to some process (Pereira, et al., 2018). The general treatment using the ohmic model with variable ionic resistivity in the formulation of D'Alkaine, et al., (2004) was applied to voltammetric data. This model allows a more detailed study of the metal/film/solution interface by the determination of the exchange current density at the metal/film interface and of the film, by the determination of values of the variable ionic resistivity of the zinc oxide film during its voltammetric growth.

2. Methodology

The working electrodes were galvanized steel sheets from two different origins, having the same coating weight of zinc. One was produced by immersion of the steel sheet in a molten zinc bath containing 0.075% antimony. The other was produced by immersion in a molten zinc bath containing 0.095% lead. It is noteworthy that before each measurement the galvanized samples were polished with 600 emery paper to provide the same roughness factor to zinc surfaces.

The electrochemical experiments were performed using an EG&G Princeton Applied Research Model 273A potentiostat. Reagents PA and purified water (Millipore Q system) were used. The electrolyte solution was 0.3 mol L^{-1} H_3BO_3 plus 0.15 mol L^{-1} $Na_2B_4O_7$, pH 8.7. This buffer solution maintains the pH at the electrode surface constant, even during the film growth. This is a necessary condition for the application of the model Equations. An acrylic electrochemical cell of 100 ml was used. The electrochemical active area of the samples sheets were 8.55 cm^2, limited by the use of an O-ring. This large

electrode area was necessary to reduce to a minimum the borders problems. The reference electrode was a $Hg/Hg_2Cl_2/KCl$ electrode in 1.0 mol L^{-1} KCl solution in a separated compartment and the counter electrode was a platinum wire.

All current and charge densities are given in terms of the geometric area of the surface of the analyzed samples.

Anodic voltammetry studies were carried out at sweep rates of 2, 5, 10, 20, 70, 100, 200, 300 and 400 mVs^{-1}, always on the same sample. For this purpose, between voltammetry and voltammetry, the grown oxide film on the previous voltammetry was reduced at a constant cathodic potential (treatment potential) equal to -1.4 V during 8 min. This was done to ensure not only the reduction of the film stuck on the surface, but also the reduction of the disrupt film adhered to it by surface tension forces (D'Alkaine, et al., 2007). At the end of this time treatment the cathodic current always stabilized at about -0.076 mA cm^{-2}. After this treatment the obtained voltammograms were reproductive. This was an indication that the surface roughness of the samples were also reproductive. To prove this, roughness measurements were made in five distinct points of the surface of each sample using a Perthometer Concept (Mahr Gmbh, Brauweg 38 Gottingen) roughness meter. The analyzed roughness parameter was the R_a (medium roughness value). The galvanized steel sheets were analyzed by (SEM) and energy dispersive X-ray spectroscopy (EDS) to verify the presence of antimony and lead in the zinc coatings.

3. Results and Discussion

3.1 Hot-dip galvanized steel sheets produced with Sb in the bath

Figure 1 presents the EDS analyzes of the hot-dip galvanized steel sheets produced with Sb in the bath which confirms the presence of Sb in the Zn coating.

Figure 1 - Characteristic EDS spectrum acquired from the galvanized steel containing Sb.
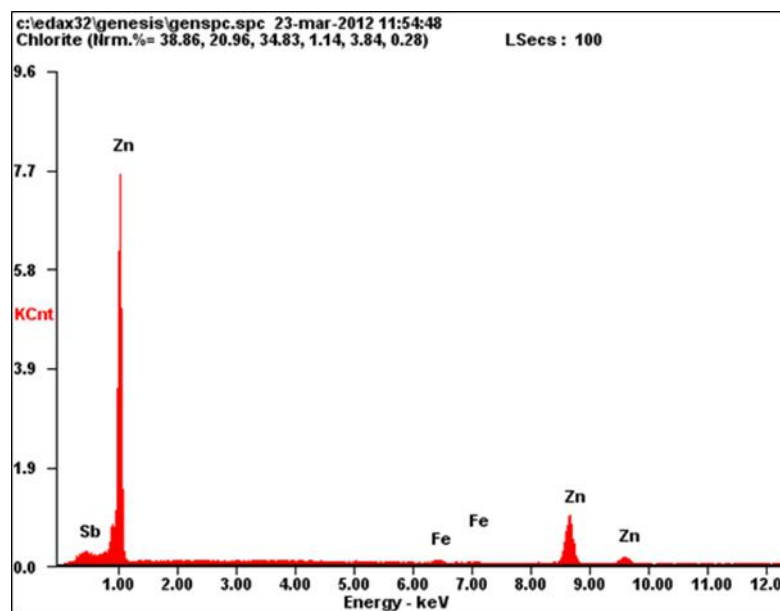

Figure 1 shows the caracterization of EDS galvanized steel sheet containing Sb. The peaks represent the elements present in the sample. The presence of Sb, Zn and Fe are observed in the galvanized steel sheet. Source: Own authors.

In Figure 2 are shown the anodic voltammograms of zinc oxide growth for hot-dip galvanized steel sheet produced with Sb in the bath. From these voltammograms the current density versus potential at the metal/film interface, i versus $E_{m/f}$ were calculated. This curve is obtained after the correction of the ohmic drop through the film (the overpotential $\eta_{f,p}$) at the

peak potential (E_p). This was done through a general treatment using the ohmic model with variable ionic resistivity (D'Alkaine, et al., 2004). The values of $\eta_{f,p}$ are calculated in this model by Equation 1

$$\eta_{f.p} = \frac{v}{i_p}(q_{f.p} + q_0)$$

(1)

where q_0 is the charge density on the metal surface related to the amount of film grown initially at the initial potential E_i of the voltammetry; v is the sweep rate potential; i_p is the current density at the peak and $q_{f,p}$ is the peak or plateau charge density.

Figure 2 - Voltammetric ZnO film growth on galvanized steel sheets with Sb.

Figure 2 presents the voltammograms at different potential sweep rates pointed out at each curve. The electrolyte solution was 0.3 molL^{-1} H$_3$BO$_3$ + 0.15 molL^{-1} Na$_2$B$_4$O$_7$; the reference electrode was Hg/Hg$_2$Cl$_2$/KCl 1.0 molL^{-1}; E$_i$ = -1.30 V. Before each voltammetry: cathodic potentiostatic electrode surface recovery at a potential of -1.4 V. Source: Own authos.

The correct value of q$_0$ is obtained by considering increasing q$_0$ values in Eq. 1 until a linear region at high v in the representation ln i$_p$ versus (E$_p$ − η$_{f,p}$) are attained. This is because the representation corresponds to the Tafel plots at the metal/film interface since the ohmic drop across the film has been corrected, show Figure 3. This linear region must be expected only for high growing sweep rates since at low sweep rates the opposite reaction is able to occur and, consequently, a deviation from linearity appears.

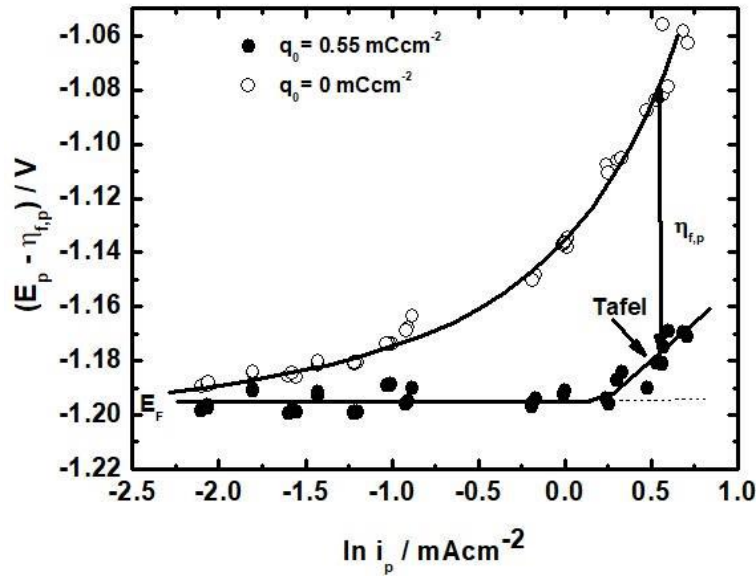**Figure 3 -** Tafel plots at the metal/film interface galvanized steel sheets with Sb.

Figure 3 shows (●) Tafel plot corrected by its ohmic drop at the Zn/ZnO interface versus the logarithm of the peak current density (Zn coating film with Sb). (○) Plot without ohmic correction for comparison. Electrolyte solution: 0.3 molL^{-1} H$_3$BO$_3$ + 0.15 molL^{-1} Na$_2$B$_4$O$_7$; reference electrode: Hg/Hg$_2$Cl$_2$/KCl 1.0 M. Source: Own authors.

In Figure 3 are shown the curves of (E$_p$ – η$_{f,p}$) vs ln i$_p$ considering q$_0$ = 0 mCcm^{-2} and q$_0$ = 0.55 mCcm^{-2}. This last one was the best adjusted value giving the more extended linear region in the Tafel plot. In Figure 4 is shown amplification of the corrected by its ohmic drop at the Zn/ZnO interface Tafel Plot from Figure 3 versus the logarithm of the peak current density (Zn film coating with Sb). q$_0$ = 0.55 mCcm^{-2}.

Figure 4 - Amplification at the Zn/ZnO interface Tafel plot from Figure 3.
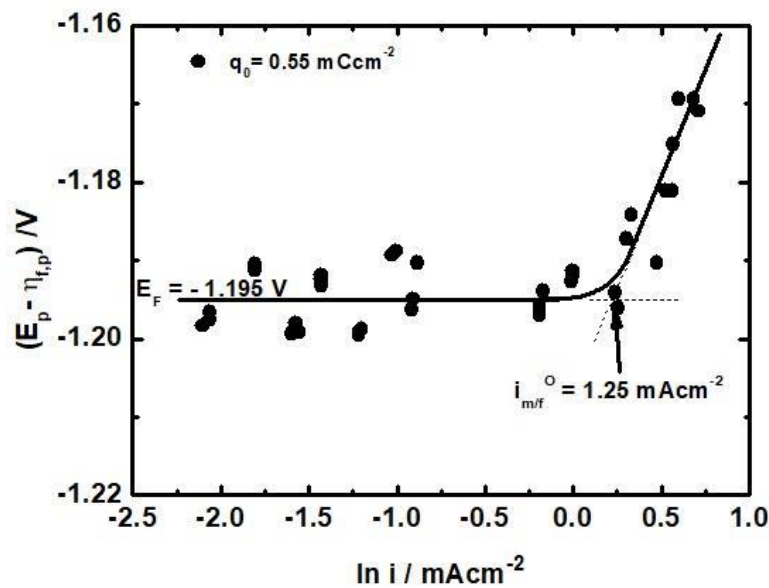

Figure 4 represents the Tafel Plot corrected by its ohmic drop at the Zn/ZnO interface from versus the logarithm of the peak current density (Zn film coating with Sb). q$_0$ = 0.55 mCcm^{-2}. E$_F$: Flade Potencial; $i_{m/f}^0$: exchange current density; α$_a$: anodic transfer coefficient, both at the metal/film interface. Electrolyte solution: 0.3 molL^{-1} H$_3$BO$_3$ + 0.15 molL^{-1} Na$_2$B$_4$O$_7$; reference electrode: Hg/Hg$_2$Cl$_2$/KCl 1.0 molL^{-1}. Source: Own authors.

In Figure 4 it is plotted only the curve obtained considering q_0 = 0.55 mCcm^{-2} in order to show the different parameters calculated from the best curve. The Flade Potential (E_F) of the galvanized steel sheets with Sb was found to be equal to -1.195 V. The Tafel slope was 53 mVdec^{-1} and the exchange current density at the Zn/ZnO interface was 1.25 mAcm^{-2}.

The transference coefficient at the Zn/ZnO interface ($\alpha_{m/f}$) could then be calculated considering

$$53mVdec^{-1} = \frac{RT}{\alpha_{m/f}F}$$

(2)

and it resulted to be 0.49.

Figure 5 shows the relation between the peak charge density of the film ($q_{f,p}$) at different potential sweep rates. It can be noticed that for sweep rates values higher than 200 mVs^{-1} (linear Tafel region in Fig. 5) the peak charge density remains constant. This means that for high sweep rates, at the peak potential, the film parameters seem to be independent of the growing conditions in the same way as found by D'Alkaine, et al., (2004) in the case of pure zinc. This is an indication of the presence of some kind of reproducible state which occurs for all passivation films studied until now when the film is grown over distinct metals at high sweep rates, (D'Alkaine & Santanna, 1998), (D'Alkaine, et al., 2004), (D'Alkaine, et al., 2007), (Motta, 2000), (Motta, 2005).

Figure 5 - The relation between the peak charge density of the film ($q_{f,p}$) at different potential sweep rates.
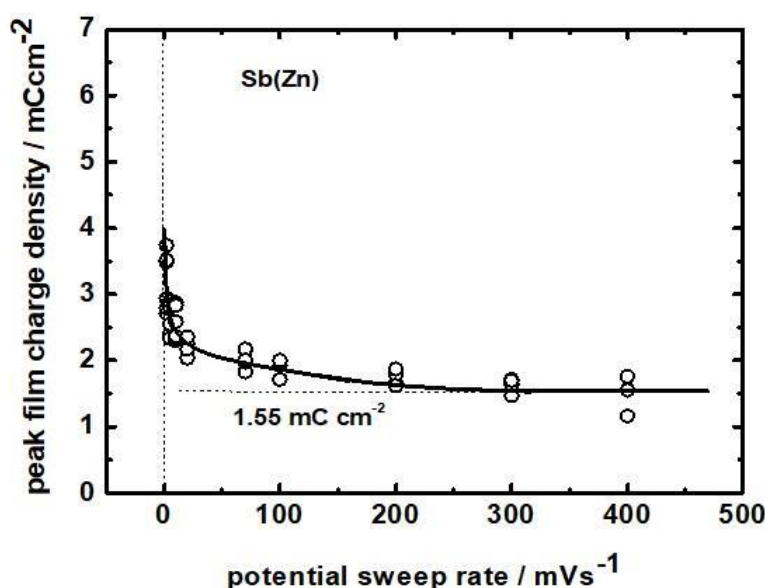

Figure 5 presents peak film charge density versus potential sweep rate. Initial charge density, q_0: 0.55 mCcm^{-2}. Electrolyte solution: 0.3 molL^{-1} H$_3$BO$_3$ + 0.15 molL^{-1} Na$_2$B$_4$O$_7$; reference electrode: Hg/Hg$_2$Cl$_2$/KCl 1.0 molL^{-1}. Soucer: Own authors.

3.2 Hot-dip galvanized steel sheets produced with Pb in the bath

Figure 6 presents the EDS analyzes of the hot-dip galvanized steel sheets produced with Pb in the bath which confirms the presence of Pb in the Zn coating.

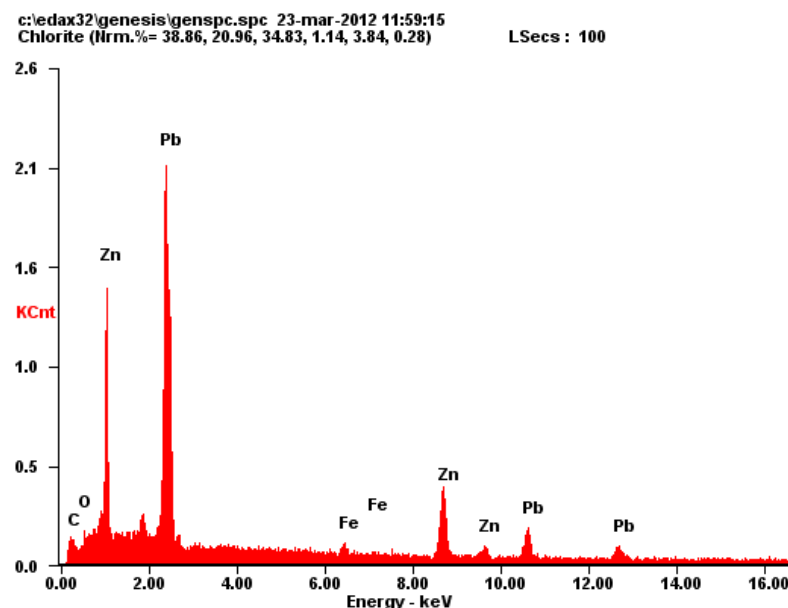**Figure 6 -** Characteristic EDS spectrum acquired from the galvanized settle with Pb.

Figure 6 shows the caracterization of EDS galvanized steel sheet containing Pb. The peaks represent the elements present in the sample. The presence of Pb, Zn and Fe are observed in the galvanized steel sheet. Source: Own authors.

The anodic voltammetries of hot-dip galvanized steel sheets samples with Pb in the coating are shown in Figure 7. These curves must be compared with those of Figure 2 for the samples with Sb addition in the bath. It is clearly seen that the charge involved in the voltammograms are larger in the case of the samples containing Pb and that these last samples present two peak processes. This could be due to an enhancing of the roughness factor during the galvanizing process (metallurgical phenomenon).

In order to elucidate this question, the roughness of both kinds of samples were experimentally measured. The value found for the hot-dip galvanized steel sheets produced with Sb in the bath was 0.21μm (R_A) while that of the hot-dip galvanized steel sheets produced with Pb in the bath presented a value of 0.25 μm (R_A). It is then possible to consider the R_A values practically equal for both samples, even further when the differences in R_A can be attributed to experimental errors. In view of this fact, the larger values of charge densities found in the voltammetries of the samples containing Pb are due to the less efficient passivating properties of the oxide grown during these experiments.

Figure 7 - Voltammetric ZnO film growth on galvanized steel sheets with Pb.
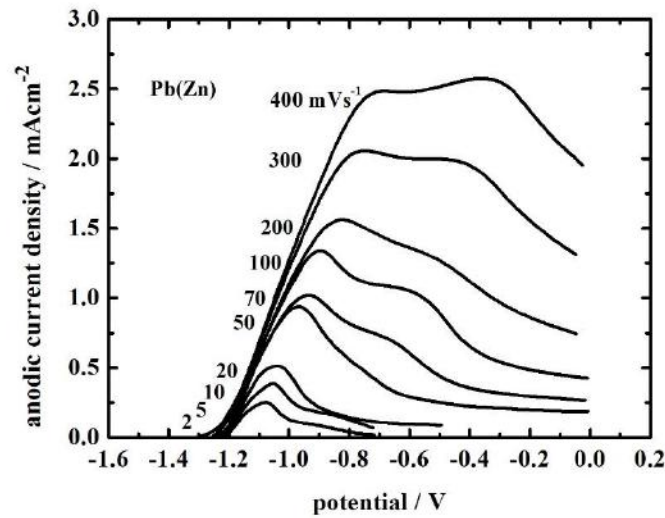

Figure 7 presents the voltammograms at different potential sweep rates pointed out at each curve. Electrolyte solution: 0.3 molL^{-1} H$_3$BO$_3$ + 0.15 molL^{-1} Na$_2$B$_4$O$_7$; reference electrode: Hg/Hg$_2$Cl$_2$/KCl 1.0 molL^{-1}; E$_i$ = -1.30 V. Before each voltammetry: cathodic potentiostatic electrode surface recovery at a potential of -1.4 V.Source: Own authors.

Following the same presentation adopted for the samples containing Sb (Figure 3), Figure 8 shows the Tafel plots for ln i$_p$ versus (E$_p$ − η$_{f,p}$) at the metal/film interface considering q$_0$ = 0 mCcm^{-2} and q$_0$ = 0.75 mCcm^{-2}. This last one was the best adjusted value giving the longer linear region for the Tafel plot. In Figure 9 is shown amplification of the corrected by its ohmic drop at the Zn/ZnO interface Tafel Plot from Figure 8 versus the logarithm of the peak current density (Zn film coating with Pb). q$_0$ = 0.75 mCcm^{-2}.

Figure 8 - Tafel plots at the metal/film interface galvanized steel sheets with Pb.
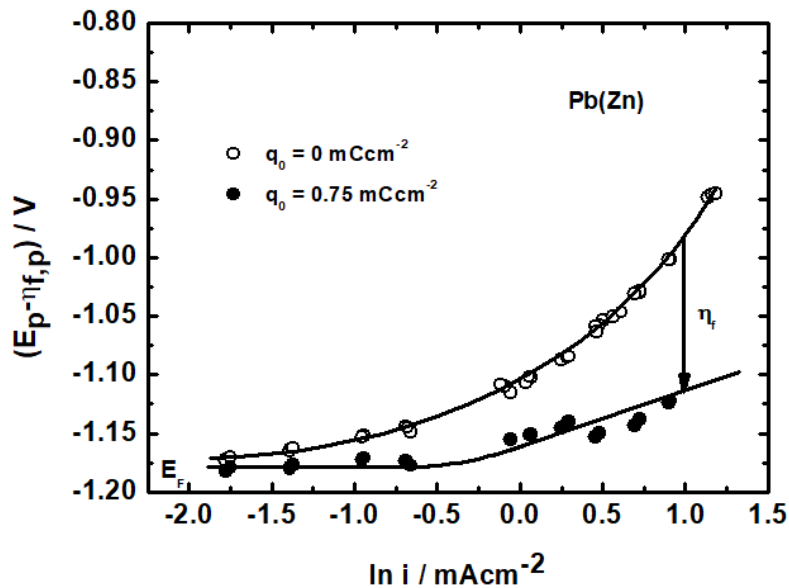

Figure 8 shows (●) Tafel plot corrected by its ohmic drop at the Zn/ZnO interface versus the logarithm of the peak current density (Zn coating film with Pb). (○) no ohmic drop corrected plot for comparison. Electrolyte solution: 0.3 molL^{-1} H$_3$BO$_3$ + 0.15 molL^{-1} Na$_2$B$_4$O$_7$; reference electrode: Hg/Hg$_2$Cl$_2$/KCl 1.0 M. Source: Own authors.

Figure 9 - Amplification at the Zn/ZnO interface Tafel plot from Figure 8.
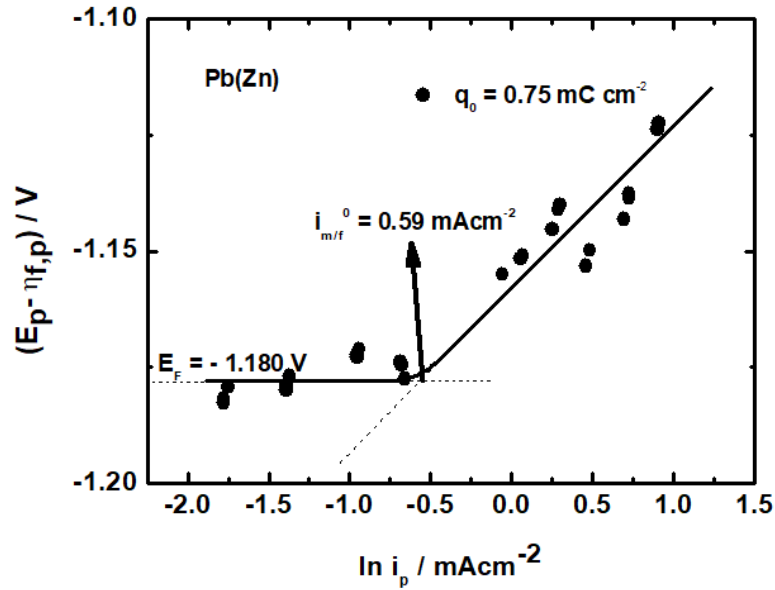

Figure 9 represents the Tafel Plot corrected by its ohmic drop at the Zn/ZnO interface from versus the logarithm of the peak current density (Zn film coating with Pb). q_0 = 0.75 mCcm^{-2}. E_F: Flade potencial; $i^0_{m/f}$: exchange current density and α_a: anodic transfer coefficient, both at the metal/film interface. Electrolyte solution: 0.3 molL^{-1} H$_3$BO$_3$ + 0.15 molL^{-1} Na$_2$B$_4$O$_7$; reference electrode: Hg/Hg$_2$Cl$_2$/KCl 1.0 molL^{-1}. Source: Own authors.

In order to better study these results, in Figure 9 only the correct Tafel plot for q_0 = 0.75 mCcm^{-2} is presented amplified in the potential scale to show the different parameter values. The Flade potential in this case was -1.18 V, very near to the E_F value found in the case of the samples containing Sb (-1.195 V), indicating that the E_F does not seem to be affected in a significant way by the presence of Sb or Pb in the zinc coating. This can be expected due to the slow amount of the Sb or Pb contents. From the extrapolation of the Tafel straight line to the Flade potential (Figure 9) it was possible to determine the exchange current density at the Zn/ZnO interface, $i^0_{m/f}$. This value was 0.590 mAcm^{-2}. It is a value little smaller, but having the same order of magnitude, than that found in the case of samples containing Sb in the coating. These facts are showing that the presence of Sb or Pb in the zinc coating does not significantly modify neither the E_F nor the $i^0_{m/f}$.

Finally, from the Tafel slope (Figure 9) it was possible to calculate the charge transfer coefficient of the oxidation reaction at the Zn/ZnO interface in the case of samples containing Pb.

In Figure 10 it is plotted the relation between the film peak charge density and the sweep rates for the hot-dip galvanized steel sheets samples with Pb in the coating. These data must be compared with those of Figure 5 related to the samples with Sb addition. From these plots the previously observed phenomena of the involved charges in the voltammetries of the samples containing Pb (Figure 10) and that containing Sb (Figure 5) confirm that the last ones are larger. This is more clearly seen at high sweep rates, were both systems attain a constant charge peak condition (1.5 mCcm^{-2} in the case of Sb and 2.60 mCcm^{-2} in the case of Pb). This result must be attributed to the film itself taking into account that no significant differences have been obtained in relation to their roughness factors. This means that the ZnO films on the surface of the samples produced in the presence of Sb in the bath are more passivating than those produced in the presence of Pb in the bath.

Figure 10 - The relation between the peak charge density of the film ($q_{f,p}$) at different potential sweep rates.
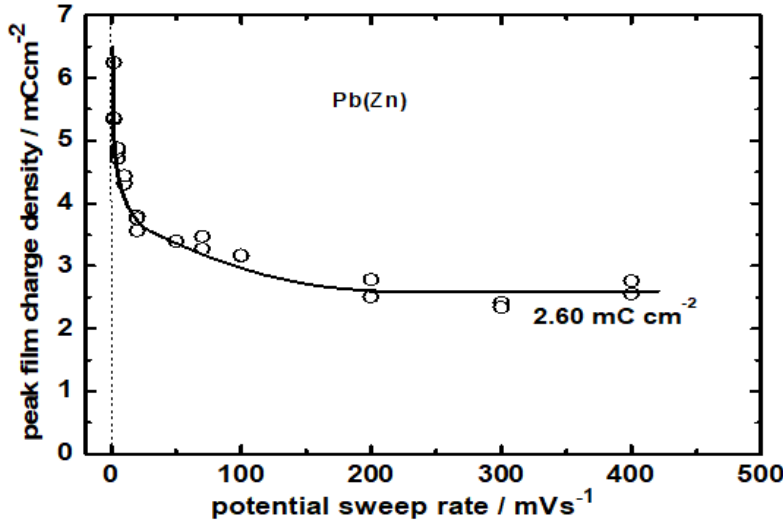

Figure 10 presents peak charge density versus the potential sweep rate. Initial charge density: 0.75 mCcm^{-2}. Electrolyte solution: 0.3 molL^{-1} H_3BO_3 + 0.15 molL^{-1} $Na_2B_4O_7$; reference electrode: Hg/Hg$_2$Cl$_2$/KCl 1.0 molL^{-1}. Source: Own authors.

If the difference is in the film, it would be important to determine some specific property of it. The general treatment including the ohmic model used in the present paper allows the determination of the ionic resistivity of the film during the growing process and not even only at the peak condition. This analyze is presented in the sequence for both systems.

From the values of the ohmic drop potential ($E_p – \eta_{f,p}$) and ln i_p in Figures 4 and 9, the curves i versus $E_{m/f}$ can be built for both cases, with Sb or Pb in the bath (Figures 11 and 12). From these Figures, it is possible to calculate the film overpotential (η_f) for any value of the charge density or current density in the film, beyond the peak conditions. This is done by determining for the same current density the difference between the potentials between the curve i versus $E_{m/f}$ and those for each sweep rate in the voltammograms (see two examples in each figure for different current densities). This procedure allows the determination of the ionic resistivity (ρ_f) during the film growth taking into account from reference D'Alkaine, et al., (2004) the following Eq.:

$$\rho_f = \frac{\eta_f}{V_f . q_f . i} \qquad (3)$$

where ρ_f is the average ionic resistivity of the film; η_f is film overpotential,; V_f is the volume per unit charge of the film; q_f is the charge density of the growing film and i is the current density.

It is worthwhile to note that the V_f value is theoretically given by Eq. 4 (D'Alkaine, et al., 2004).

$$V_f = \frac{M}{n.F.\delta} \qquad (4)$$

where M is the molecular weight of the film; $n.F$ is the charge needed to the formation of one mol of the film, with F the Faraday constant and δ the ZnO film density (6.06 g.cm^{-3}).

As stated before, the determination of each η_f for each i during a voltammetry is made from the differences between the specific curves given in Figures 11 and 12.

Figure 11 - Voltammetric growths of ZnO on galvanized steel sheets containing Sb.
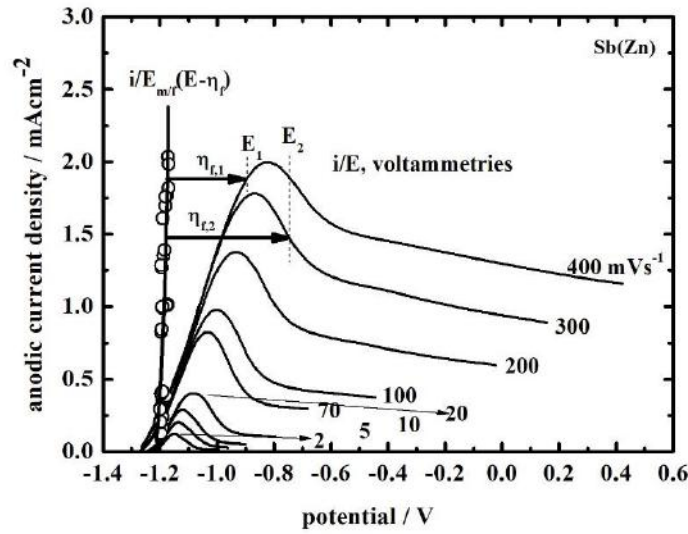

Figure 11 presents the voltammetric growths of ZnO on galvanized steel sheets containing Sb togheter with the plot of the calculated $i / (E − \eta_f)$ relation at the metal/film interface, considering $q_0 = 0.55$ $mCcm^{-2}$ and from Figure 3. Electrolyte solution: 0.3 $molL^{-1}$ H_3BO_3 + 0.15 $molL^{-1}$ $Na_2B_4O_7$; reference electrode: $Hg/Hg_2Cl_2/KCl$ 1.0 $molL^{-1}$. Source authors.

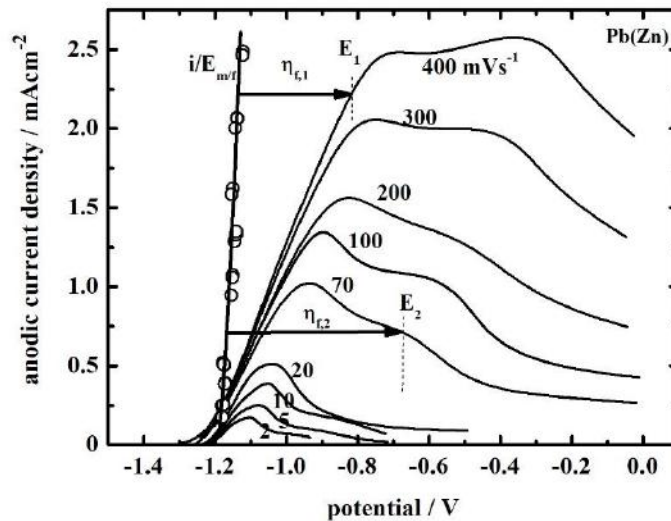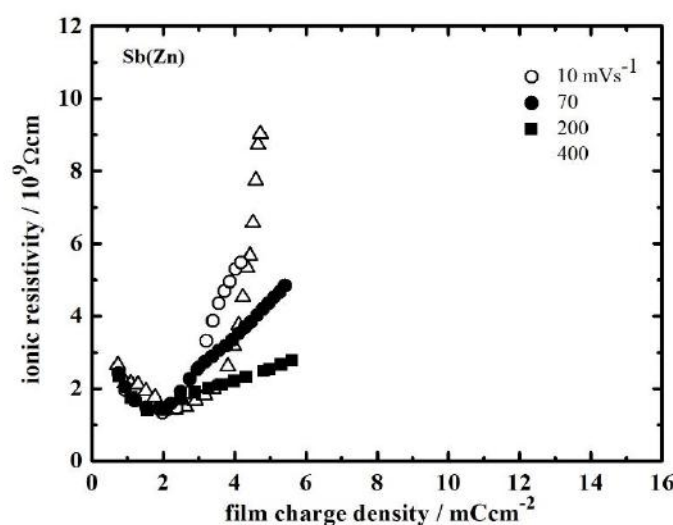**Figure 12** - Voltammetric growths of ZnO on galvanized steel sheets containing Pb.

Figure 12 presents the voltammetric growths of ZnO on galvanized steel sheets containing Pb together with the plot of the calculated $i /(E − \eta_f)$ relation at the metal/film interface, considering $q_0 = 0.75$ $mCCm^{-2}$ and from Figure 7. Electrolyte solution: 0.3 $molL^{-1}$ H_3BO_3 + 0.15 $molL^{-1}$ $Na_2B_4O_7$; reference electrode: $Hg/Hg_2Cl_2/KCl$ 1.0 $molL^{-1}$. Source authors.

From Figures 11 and 12 the variation of the ionic resistivity during the growth of both films were calculated. These results are shown in Figures 13 and 14. It can be observed that in both cases of Figures 13 and 14 the ionic resistivity of the films passes through a minimum which corresponds to the maximum in terms of current density in voltammetric Figures 2 and 7. This has been explained by the passage of the current in the initial thin aged film, having a thickness equal to q_0. This generates the injection of recombining point defects and, consequently, the decrease of the ionic resistivity (inversely
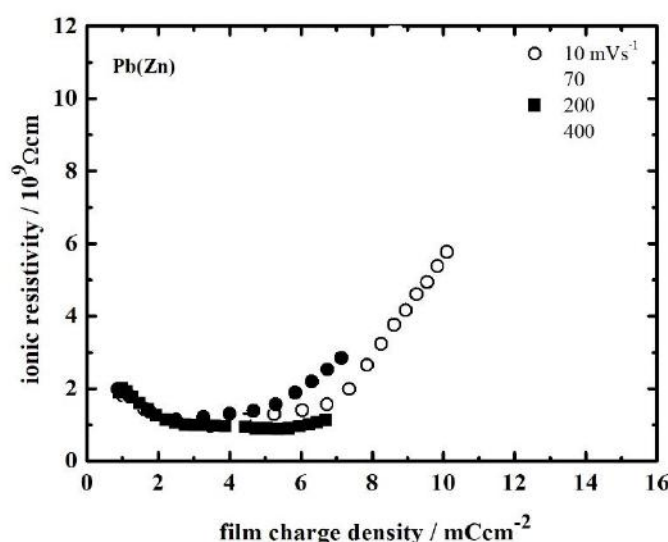
proportional to the concentration of point defects). On the order hand, the growth of the concentration of recombining point defects (interstitials cations and cationic vacancies) in the film lead to the recombination reaction (interstitial cation + cationic vacancies → lattice) originating, subsequently, the growth of the ionic resistivity, generating the minimum (D'Alkaine & Santanna, 1998), (D'Alkaine, et al., 2004), (D'Alkaine, et al., 2007), (Boscheto, 2008), (D'Alkaine, et al., 1993).

Figure 13 - Ionic resistivity vs. film charge density for different sweep rates indicated in the figure. The case of galvanized steel with Sb. Electrolyte solution: 0.3 molL^{-1} H$_3$BO$_3$ + 0.15 molL^{-1} Na$_2$B$_4$O$_7$; reference electrode: Hg/Hg$_2$Cl$_2$/KCl 1.0 molL^{-1}.

Source Authors.

Figure 14 - Ionic resistivity vs. film charge density for different sweep rates indicated in the figure. The case of galvanized steel with Pb. Electrolyte solution: 0.3 molL^{-1} H$_3$BO$_3$ + 0.15 molL^{-1} Na$_2$B$_4$O$_7$; reference electrode: Hg/Hg$_2$Cl$_2$/KCl 1.0 molL^{-1}.

Source Authors.

It is worthwhile to notice that hot-dip galvanized steel sheets produced with Sb in the bath present less corrosion than those produced with Pb in the bath. This fact can be explained comparing the ionic resistivity values of both samples, in the

same sweep rate. The data show that the ionic resistivity becomes up more quickly, leading to more efficient passivation, in the case of the hot-dip galvanized steel sheets produced with Sb than those with Pb, in agreement with the corrosion results.

4. Conclusion

Two galvanizing steel cases were analyzed from the point of view of their passivating films. One produced with the addition of antimony in the bath and the other with the addition of Pb.

It was observed in both cases in the voltammetric results a similar behavior of passivating films of those in pure zinc. It was possible to verify that in the Zn/ZnO interface the oxidation processes in both cases, with Sb or with Pb in the bath, follow a process which can be described by a Tafel reaction and that the Flade Potential and the transfer coefficient do not varied with the presence of Sb or Pb in the bath. Nevertheless, the exchange current at the Zn/ZnO in the case of the system containing Sb in the bath is near a half of the value of that corresponding to the sample containing Pb in the bath. This is a first indication that the presence of Sb in the bath in comparison with Pb generates a more anticorrosive film. This date can be confirmed by the determination of the ionic resistivities of the films during the film growths, which indicate that the films with Sb arrives to passivate the metal more easily than those with Pb.

References

Asgari, H., Toroghinejad, M. R., & Golozar, M. A. (2007). On texture, corrosion resistence and morphology of hot-dip galvanized zinc coatings. *Applied Surface Science, 253*, pp. 6769 - 6777.10.1016/j.apsusc.2007.01.093

Asgari, H., Toroghinejad, M. R., & Golozar, M. A. (2009). Effect of coatings thickness on modifyind the texture and corrosion performace of hot-dip galvanized coatings. *Current Applied Physics, 9*, pp. 59 - 66.10.1016/j.cap.2007.10.090

Boscheto, E. P. (2008). Simulação do crescimento de filmes sobre metais. O caso voltamétrico. Dissertação (Mestrado) – Universidade Federal de São Carlos. São Carlos, São Paulo, pp. 1-69.

Cameron, D. J., Harvey, G. J., & Ormay, M. K. (1965). The spangle of galvanized iron. *Journal Australian Institute of Metals, 10*, p. 225.

Chang, S., & Shin, J. C. (1994). The effect of antimony additions on hot dip coatings. *Corrosion Science, 36*, pp. 1425-1436.10.1016/0010-938X(94)90190-2

D'Alkaine, C. V., & Santanna, M. A. (1998). Passivating films on nickel in alkaline solutions II. Ni(II) anodic film growth: quantitative treatment and the influence of the OH⁻ concentration. *Journal of Electroanalytical Chemistry, 457*, 13-21.10.1016/S0022-0728(98)00227-7

D'Alkaine, C. V., Garcia, C. M., Brito, G. A., Pratta, P. M., & Fernandes, F. P. (2007). Disruption processes in films grown and reduced electrochemically on metals. *Journal of Solid State Electrochemistry, 11*, 1575-1583.10.1007/s10008-007-0361-x

D'Alkaine, C. V., Souza, L. M., & Nart, F. C. (1993). The anodic behaviour of niobium—II. General experimental electrochemical aspects. *Corrosion Science, 34*, 117-127.10.1016/0010-938X(93)90263-G

D'Alkaine, C. V., Tulio, P. C., & Berton, M. A. (2004). Quantitative Ohmic model for transient growths of passivating films: The voltammetric case. *Electrochimica Acta, 49*, 1989-1997.10.1016/j.electacta.2003.12.029

Fedel, M., Olivier, M., Poelman, M., Deflorian, F., Rossi, S., & Druart, M. -E. (2009). Corrosion protection properties of silane pre-treated powder coated galvanized steel. *Progress in Organic Coatings, 66*, 118-128.10.1016/j.porgcoat.2009.06.011

Hamlaoui, Y., Tifouti, L., & Pedraza, F. (2009). Corrosion behaviour of molybdate–phosphate–silicate coatings on galvanized steel. *Corrosion Science, 51*, 2455-2462.10.1016/j.corsci.2009.06.037

Hosseini, M., Ashassi-Sorkhabi, H., & Ghiasvand, H. A. (2007). Corrosion protection of electro-galvanized steel by green conversion coatings. *Journal of Rare Earths, 25*, 537-543.10.1016/S1002-0721(07)60558-4

Kobayashi, Y., & Fujiwara, Y. (2006). Effect of SO_4^{-2} on the corrosion behavior of cerium-based conversion coatings on galvanized steel. *Electrochimica Acta, 51*, pp. 4236-4242.10.1016/j.electacta.2005.11.043

Lin, B., Lu, J., Kong, G., & Liu, J. (2007). Growth and corrosion resistance of molybdate modified zinc phosphate conversion coatings on hot-dip galvanized steel. *Transactions of Nonferrous Metals Society of China, 17*, 755-761.10.1016/S1003-6326(07)60169-1

Marder, A. R. (2000). The Metallurgy of zinc-coated steel. *Progress in Materials Science, 45*, pp. 191 - 271.10.1016/S0079-6425(98)00006-1

Meng, G., Zhang, L., Shao, Y., Zhang, T., Wang, F., Dong, C., & Li, X. (2009). Effect of refining grain size on the corrosion behavior of Cr(III) conversion layers on zinc coatings. *Scripta Materialia, 61*, 1004-1007.10.1016/j.scriptamat.2009.08.004

Motta, H. N. (2000). Crescimento de óxido de cádmio sobre cádmio em meio alcalino. Dissertação (Mestado) – Universidade Federal do Paraná. Curitiba, Paraná, pp. 1-174.

Motta, H. N. (2005). Estudo da cinética de crescimento de óxidos sobre metais. O caso do cádmio em meio alcalino. Tese (Doutorado) – Universidade Federal do Paraná. Curitiba, Paraná, pp. 1-214.

Pereira, A. S., Shitsuka, D. M., Parreira, F. J., & Shitsuka, R. (2018). Metodologia da pesquisa científica. UFSM. https://repositorio.ufsm.br/handle/1/15824

Ramezanzadeh, B., Attar, M. M., & Farzam, M. (2010). Corrosion performance of a hot-dip galvanized steel treated by different kinds of conversion coatings. *Surface and Coatings Technology, 205*, 874-884.10.1016/j.surfcoat.2010.08.028

Seré, P. R., Culcasi, J. D., Elsner, C. I., & Di Sarli, A. R. (1999). Relationship between texture and corrosion resistence in hot-dip galvanized steel sheets. *Surface and Coatings Technology, 122*, pp. 143 - 149.10.1016/S0257-8972(99)00325-4

Taouil, A. E., Mahmoud, M. M., Lallemand, F., Lallemand, S., Gigandet, M.-P., & Hin, J.-Y. (2012). Corrosion protection by sonoelectrodeposited organic films on zinc coated steel. *Ultrasonics Sonochemistry, 19*, 1186-1193.10.1016/j.ultsonch.2012.03.005

Tomachuk, C. R., Melo, H. G., & Bellucci, F. (2006). Estudo de filmes orgânicos aplicados em eletrozincados passivados isentos de cromo hexavalente. *17° CEBECIMat*. Foz do Iguaçú, Paraná, Brasil.